Contribution from the Department of Chemistry and Biochemistry, University of Colorado, Boulder, Colorado 80309

Catecholate Complexes of High-Oxidation-State Metal Ions. Synthesis and Characterization of Dimeric Hexakis(tetrachlorocatecholato)ditungsten(VI)

Lynn A. deLearie and Cortlandt G. Pierpont*

Received April 5, 1988

The thermal reaction between $W(CO)_6$ and tetrachloro-1,2-benzoquinone in toluene produces the tris(quinone)tungsten complex isolated as the toluene solvate. Crystals of this complex have been characterized structurally. As the toluene solvate, $W(O_2C_6Cl_4)_3 \cdot 1.5C_6H_5CH_3$ crystallizes in the monoclinic space group $C2/c$, with unit cell dimensions of a = 22.595 (5) Å, b = 11.830 (3) Å, c = 27.126 (7) Å, β = 101.61 (2)°, and Z = 8. The complex molecule was found to be dimeric, located along a 2-fold axis of the unit cell, with two quinone ligands chelated to each metal ion and two quinones bridging adjacent metal ions. Features of the molecule indicate that the quinones are coordinated as catecholate ligands and that the metal ions are W(VI). Toluene solvate molecules stack between catecholate ligands of adjacent $W_2(Cl_4Cat)_6$ molecules, forming an extended network structure in the solid state. The dark brown tungsten complex and its purple molybdenum analogue show intense absorptions in the visible region and show bands characteristic of catecholate ligands in the infrared region that further verify the charge distribution. Cyclic voltammograms on both complexes show three reversible two-electron reductions at the metals and irreversible oxidations at the catecholate ligands.

Introduction

As strong σ and π donors, the catecholate ligands are able to form complexes with metal ions in unusually high oxidation states. Treatment of $Re_2(CO)_{10}$ with tetrachloro-1,2-benzoquinone (Cl_4BQ) in either thermal or photochemical reactions produced $Re^{VI}(Cl_4Cat)_3$.[1] Examples of Re(VI) are rare, and complexes that lack oxo or nitrido ligands are confined to the air- and moisture-sensitive hexamethylrhenium(VI) and hexafluororhenium(VI) species. It was of interest to extend this study to tungsten. Tungsten(VI) phenoxide complexes have been of considerable interest as catalyst precursors in olefin metathesis reactions,[2] and the halogenated aryloxide complexes have been found to be particularly active.[3] In a report that is pertinent to our present investigation, McNelis indicated that combinations of (mesitylene)$W(CO)_3$ and Cl_4BQ could be used in catalytic metathesis reactions.[4]

We reported earlier that reaction between $Mo(CO)_6$ and Cl_4BQ gave the $Mo^{VI}_2(Cl_4Cat)_6$ dimer.[5] Infrared spectra of this complex and of $Re(Cl_4Cat)_3$ are quite similar and show no obvious features that might be associated with the structural difference. In this report we describe the reaction between $W(CO)_6$ and Cl_4BQ. The product of this reaction has been characterized structurally to establish similarity with either the Re or Mo analogues, and both the Mo and W complexes have been studied spectrally and electrochemically.

Experimental Section

$W(CO)_6$ and $Mo(CO)_6$ were obtained from Strem Chemical Co., and tetrachloro-1,2-benzoquinone was obtained from Aldrich Chemical Co. All reagents were used as received; all reactions were carried out in freshly distilled solvents by standard Schlenk-line techniques.

$W_2(Cl_4Cat)_6 \cdot 3C_6H_5CH_3$. Tetrachloro-1,2-benzoquinone (1.48 g; 6.0 mmol) and $W(CO)_6$ (0.68 g; 1.9 mmol) were dissolved in 60 mL of toluene, and the solution was refluxed for 24 h under N_2. The crystalline product was obtained from the solution in essentially quantitative yield by slow evaporation of the solvent.

$Mo_2(Cl_4Cat)_6 \cdot 3C_6H_6$. Samples of $Mo_2(Cl_4Cat)_6$ were prepared by the general procedure as described above for tungsten and as reported earlier.[5] Benzene was used as the solvent in this reaction, and the complex was obtained as the benzene solvate.

Physical Measurements. Infrared spectra were recorded on a Beckman IR 4250 spectrometer and on an IBM IR/30 FTIR spectrometer with samples prepared as KBr pellets. UV-vis spectra were recorded on a Hewlett Packard 8451A diode array spectrophotometer. Cyclic voltammograms were obtained with a BAS-100 electrochemical analyzer. A platinum-disk working electrode and a platinum-wire counter electrode were used. The reference electrode was based on the Ag/Ag^+ couple and consisted of a silver hexafluorophosphate solution (CH_2Cl_2) in contact with a silver wire placed in glass tubing with a Vycor frit at one end to allow ion transport. Tetrabutylammonium hexafluorophosphate was used as the supporting electrolyte, and the ferrocene/ferrocenium couple was used as an internal standard.

Table I. Crystal Data and Details of the Structure Determination and Refinement for $W_2(O_2C_6Cl_4)_6 \cdot 3C_6H_5CH_3$

formula	$W_2O_{12}C_{57}H_{24}Cl_{24}$	Z	4
mol wt	2119.38	T, K	294-296
space group[a]	$C2/c$	λ, Å	0.71069 (Mo Kα)
a, Å[b]	22.595 (5)	ρ_{meas}, g/cm^3[c]	1.95 (2)
b, Å	11.830 (3)	ρ_{calc}, g/cm^3	1.98
c, Å	27.126 (7)	μ, cm^{-1}	43.90
β, deg	101.61 (2)	transmission factors	0.931, 0.592
V, Å^3	7102 (2)	R, R_w[d] (obsd data)	0.0365, 0.0465

[a] *International Tables for X-ray Crystallography*; Kynoch: Birmingham, England, 1965; Vol. 1. [b] Cell dimensions were determined by least-squares fit of the setting angles for 20 reflections with 2θ in the range 20-30°. [c] By flotation in $ZnBr_2$. [d] The quantity minimized in the blocked-cascade least-squares procedures is $\sum w(|F_o| - |F_c|)^2$. $R = R_1 = \sum||F_o| - |F_c||/\sum|F_o|$; $R_w = R_2 = [\sum w(|F_o| - |F_c|)^2/\sum w(F_o)^2]^{1/2}$.

Crystallographic Structure Determination on $W_2(O_2C_6Cl_4)_6 \cdot 3C_6H_5CH_3$. A black-brown crystal of the complex was mounted and coated with an amorphous resin to prevent loss of solvent and crystal deterioration during data collection. Photographs indicated monoclinic symmetry. Unit cell dimensions given in Table I were calculated from the centered settings of 20 intense reflections with 2θ values greater than 20°. Details of procedures used for data collection and structure determination are given in Table I.

The position of the W atom was determined from a three-dimensional Patterson map. Phases derived from the W position were used to obtain positions of the 12 chlorine atoms, and the W and Cl atoms were used to determine positions of all other atoms of the structure. The 1.5 independent toluene solvate molecules of the structure are present as three half-molecules, located about positions of symmetry in the unit cell. Two are located about inversion centers at $^1/_2$, $^1/_2$, 0 and $^1/_4$, $^1/_4$, 0; the third is located about the 2-fold axis at 0, y, $^3/_4$, which relates the halves of the dimeric complex molecule. Methyl carbon atoms were found to be disordered, and the solvate phenyl rings were refined as rigid groups. Final cycles of refinement converged with discrepancy indices of R = 0.037 and R_w = 0.047. Maximum residual electron density of 0.89 e/Å^3 was found in the vicinity of the toluene solvate molecule located about the 2-fold axis. Final positional parameters for the $W_2(Cl_4Cat)_6$ complex molecule are listed in Table II. Tables containing positional and anisotropic thermal parameters for atoms of the structure, least-squares planes and dihedral angles, and observed and calculated structure factors obtained from refinement are available as supplementary material.

Experimental Results

The thermal reaction between $W(CO)_6$ and tetrachlorobenzoquinone produced the dark brown tris(quinone)tungsten product in high yield. Similar procedures were used to form the

(1) deLearie, L. A.; Haltiwanger, R. C.; Pierpont, C. G. *Inorg. Chem.* **1987**, *26*, 817.
(2) (a) Hocker, H.; Musch, R.; Jones, F. R.; Luederwald, I. *Angew. Chem., Int. Ed. Engl.* **1973**, *12*, 430. (b) Dodd, H. T.; Rutt, K. J. *J. Mol. Catal.* **1985**, *28*, 33.
(3) (a) Quignard, F.; Leconte, M.; Basset, J.-M. *J. Mol. Catal.* **1985**, *28*, 27. (b) Quignard, F.; Leconte, M.; Basset, J.-M. *J. Mol. Catal.* **1986**, *36*, 13.
(4) Taneja, R.; McNelis, E. *Oxid. Commun.* **1984**, *7*, 191.
(5) Pierpont, C. G.; Downs, H. H. *J. Am. Chem. Soc.* **1975**, *97*, 2123.

0020-1669/88/1327-3842$01.50/0 © 1988 American Chemical Society

Table II. Atomic Coordinates ($\times 10^4$) and Equivalent Isotropic Displacement Parameters ($Å^2 \times 10^3$)

	x/a	*y/b*	*z/c*	*U*(eq)[a]
W	566 (1)	2290 (1)	−1683 (1)	34 (1)
O1	−713 (2)	1912 (4)	−2668 (2)	38 (1)
O2	−82 (2)	3250 (4)	−1938 (2)	40 (1)
O3	−115 (2)	1361 (3)	−1587 (2)	38 (1)
O4	950 (2)	911 (4)	−1407 (2)	43 (1)
O5	1241 (2)	3305 (4)	−1708 (2)	40 (1)
O6	710 (2)	2989 (4)	−1025 (2)	44 (2)
C1	−1013 (3)	2473 (4)	−2367 (2)	34 (2)
C2	−1631 (3)	2340 (6)	−2407 (3)	50 (2)
C3	−1933 (3)	2982 (6)	−2096 (3)	50 (3)
C4	−1614 (3)	3697 (7)	−1739 (3)	56 (3)
C5	−992 (3)	3781 (6)	−1677 (3)	48 (2)
C6	−697 (3)	3171 (5)	−1999 (2)	38 (2)
C7	−4 (3)	304 (5)	−1406 (2)	39 (2)
C8	−436 (3)	−465 (5)	−1344 (3)	42 (2)
C9	−242 (3)	−1540 (6)	−1184 (3)	50 (2)
C10	367 (3)	−1816 (6)	−1092 (3)	53 (3)
C11	797 (3)	−1022 (6)	−1153 (3)	48 (2)
C12	604 (2)	47 (5)	−1307 (2)	39 (2)
C13	1439 (3)	3981 (5)	−1313 (2)	41 (2)
C14	1905 (3)	4753 (6)	−1278 (3)	50 (2)
C15	2061 (3)	5365 (6)	−829 (3)	54 (3)
C16	1755 (3)	5225 (6)	−440 (3)	54 (2)
C17	1289 (3)	4443 (6)	−486 (3)	51 (2)
C18	1135 (3)	3814 (5)	−927 (2)	42 (2)
Cl1	−2010 (1)	1387 (2)	−2826 (1)	70 (1)
Cl2	−2704 (1)	2904 (2)	−2181 (1)	92 (1)
Cl3	−1982 (1)	4482 (3)	−1362 (1)	97 (1)
Cl4	−570 (1)	4591 (2)	−1217 (1)	85 (1)
Cl5	−1181 (1)	−93 (2)	−1478 (1)	71 (1)
Cl6	−769 (1)	−2533 (2)	−1096 (1)	85 (1)
Cl7	592 (1)	−3163 (2)	−898 (1)	94 (1)
Cl8	1556 (1)	−1339 (2)	−1035 (1)	86 (1)
Cl9	2272 (1)	4881 (2)	−1767 (1)	74 (1)
Cl10	2648 (1)	6323 (2)	−771 (1)	88 (1)
Cl11	1940 (1)	6017 (2)	93 (1)	90 (1)
Cl12	879 (1)	4241 (2)	−19 (1)	79 (1)

[a] Equivalent isotropic *U* defined as one-third of the trace of the orthogonalized U_{ij} tensor.

molybdenum[5] and rhenium[1] analogues; all were obtained in the form of solvates. These complexes are air stable and show no unusual moisture sensitivity. However, over the period of weeks in a container open to the atmosphere, all were observed to form colorless fibers that were identified by mass spectrometry as tetrachlorocatechol. This may result from slow hydrolysis of the complexes by moisture in the air to form an oxometallic product and the catechol. Intractable black materials are obtained as the metal-containing products of these decomposition reactions.

Crystallographic Characterization of $W_2(Cl_4Cat)_6$. The dimeric $W_2(Cl_4Cat)_6$ complex molecule is located about a crystallographic 2-fold axis in the unit cell. Drawings showing the inner coordination sphere and the solvate structure are given in Figures 1 and 2. A stereoview is available with the supplementary material. Bond distances and angles are given in Table III. Tungsten atoms of the molecule are each chelated by two tetrachlorocatecholate ligands and are bridged by two catecholate ligands that bond to the metals through outer electron pairs on the oxygen atoms. Tungsten–oxygen lengths involving the chelated oxygen atoms range from 1.926 (4) to 1.951 (4) Å, with the longest values involving oxygens O3 and O5, which are directly trans to one another. Shorter values are involve oxygens O4 and O6, which are approximately trans to oxygens of the bridging ligands. Oxygens O1 and O2 have the shortest W–O lengths of the structure, with values of 1.910 (4) and 1.873 (4) Å. However, these values are longer than W–O lengths reported for the aryloxide complexes $W(OAr)_4Cl_2$ and $W(OAr)_2Cl_4$, which range from 1.82 to 1.85 Å.[6] The dihedral angle between planes of bridging ligands is 78.7°, and the W–W separation is 4.653 (1) Å. Carbon–oxygen lengths of the ligands are in the 1.34–1.35-Å range expected for catecholate ligands,[7] and ring C–C lengths are

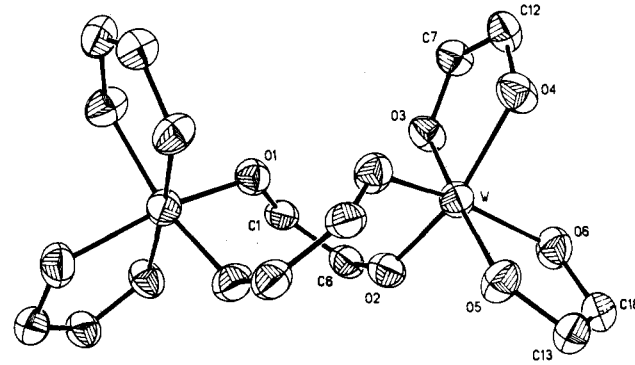

Figure 1. View of the inner coordination geometry of the $W_2(Cl_4Cat)_6$ molecule. The dihedral angle between planes of bridging ligands is 78.7°.

Table III. Selected Bond Lengths (Å) and Angles (deg)

Bridging Ligand			
Bond Lengths			
W–O1A[a]	1.910 (4)	C4–C5	1.383 (10)
W–O2	1.873 (4)	C5–C6	1.401 (10)
O1–C	1.338 (7)	C6–C1	1.379 (8)
O2–C6	1.368 (7)	Cl1–C2	1.704 (7)
C1–C2	1.388 (9)	Cl2–C3	1.713 (7)
C2–C3	1.409 (11)	Cl3–C4	1.717 (9)
C3–C4	1.376 (10)	Cl4–C5	1.705 (7)
Bond Angles			
WA–O1–C1	130.5 (4)	O1–C1–C6	119.1 (5)
W–O2–C6	134.6 (4)	O2–C6–C5	119.2 (5)
O1–C1–C2	121.4 (5)	O2–C6–C1	119.6 (6)
Chelated Ligand 1			
Bond Lengths			
W–O3	1.951 (4)	C10–C11	1.384 (10)
W–O4	1.926 (4)	C11–C12	1.374 (9)
O3–C7	1.348 (7)	C12–C7	1.381 (8)
O4–C12	1.348 (7)	Cl5–C8	1.706 (6)
C7–C8	1.368 (9)	Cl6–C9	1.723 (7)
C8–C9	1.386 (9)	Cl7–C10	1.723 (7)
C9–C10	1.387 (10)	Cl8–C11	1.722 (6)
Bond Angles			
W–O3–C7	118.5 (3)	O3–C7–C12	112.3 (5)
W–O4–C12	119.2 (3)	O4–C12–C11	126.8 (5)
O3–C7–C8	125.2 (5)	O4–C12–C7	112.8 (5)
Chelated Ligand 2			
Bond Lengths			
W–O5	1.951 (4)	C16–C17	1.390 (10)
W–O6	1.934 (4)	C17–C18	1.391 (9)
O5–C13	1.340 (7)	C18–C13	1.376 (10)
O6–C18	1.358 (7)	Cl9–C14	1.706 (8)
C13–C14	1.383 (9)	Cl10–C15	1.729 (7)
C14–C15	1.399 (10)	Cl11–C16	1.702 (7)
C15–C16	1.382 (11)	Cl12–C17	1.731 (8)
Bond Angles			
W–O5–C13	118.4 (4)	O5–C13C18	112.7 (5)
W–O6–C18	117.9 (4)	O6–C18–C17	126.6 (6)
O5–C13–C14	125.2 (6)	O6–C18–C13	113.3 (5)
Angles about Metal			
O1A–W–O2	94.0 (2)	O2–W–O6	93.1 (2)
O1A–W–O3	106.1 (2)	O3–W–O4	77.1 (2)
O1A–W–O4	90.6 (2)	O3–W–O5	173.6 (2)
O1A–W–O5	80.2 (2)	O3–W–O6	96.3 (2)
O1A–W–O6	157.4 (2)	O4–W–O5	103.9 (2)
O2–W–O3	79.1 (2)	O4–W–O6	91.4 (2)
O2–W–O4	156.1 (2)	O5–W–O6	77.4 (2)
O2–W–O5	99.9 (2)		

[a] Type A atoms of the dimer are related to those in Table II by the crystallographic 2-fold rotation of the space group.

(6) (a) Quignard, F.; Leconte, M.; Basset, J.-M.; Hsu, L.-Y.; Alexander, J. J.; Shore, S. G. *Inorg. Chem.* **1987**, *26*, 4272. (b) Handy, L. B.; Fair, C. K. *Inorg. Nucl. Chem. Lett.* **1975**, *11*, 496.

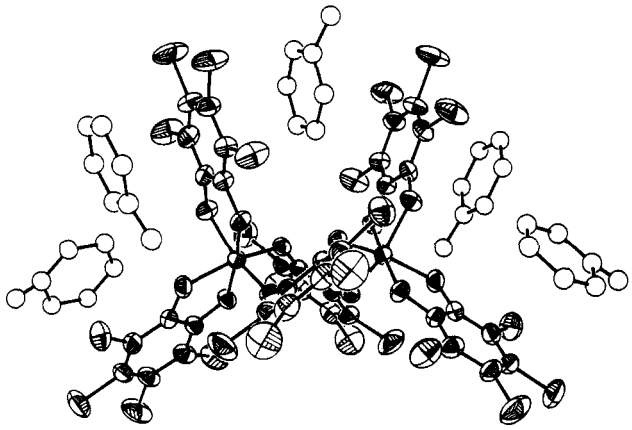

Figure 2. View of $W_2(Cl_4Cat)_6 \cdot 3C_6H_5CH_3$. Toluene methyl carbon atoms are shown in one disordered site.

reflective of their aromatic character.

The toluene solvate structure shown in Figure 2 is essentially the same as the benzene solvate structure of $Mo_2(Cl_4Cat)_6 \cdot 3C_6H_6$.[5] The molecule at the upper center of the figure is bisected by the 2-fold axis that relates the halves of the complex molecule. It is located between planes of two catecholate ligands. The other toluene solvate molecules shown in the figure are located about crystallographic inversion centers and are paired with catecholate ligands. With the centers of symmetry, they are sandwiched between ligands of adjacent complex molecules, forming an extended network structure in the crystal lattice.

Spectroscopic Properties of $Mo_2(Cl_4Cat)_6$ and $W_2(Cl_4Cat)_6$. Infrared spectra of the tetrachlorocatecholate complexes are similar in the 1000–1600-cm^{-1} region and characteristic of charge distribution within these complexes. The tetrachlorosemiquinone complexes $M(Cl_4SQ)_3$ (M = V, Cr, Fe) show a strong, broad envelope of bands in the 1480-cm^{-1} region, while the tetrachlorocatecholate complexes $V(Cl_4Cat)_3^-$, $Re(Cl_4Cat)_3$, $Mo_2(Cl_4Cat)_6$, and $W_2(Cl_4Cat)_6$ show similar spectra with an intense envelope of bands in the 1250-cm^{-1} region.[1,8] Major features in the spectrum of the tungsten complex above 800 cm^{-1} include bands of strong intensity at 1395, 1273, 1260, 1006, 842, and 824 cm^{-1}, with bands of medium intensity at 1559, 1470, and 1211 cm^{-1}. There is no obvious feature in the spectra of the W and Mo complexes that can be uniquely related to their dimeric structures. Their spectra bear close similarity in band positions and intensities to the spectra of both monomeric vanadium and rhenium tetrachlorocatecholate complexes.

Electronic spectra of both $Mo_2(Cl_4Cat)_6$ and $W_2(Cl_4Cat)_6$ recorded under an atmosphere of nitrogen show solvent dependence and spectral changes that occur with time after solution preparation. Bands that are characteristic of the W complex occur at 418 nm (ϵ 31 000 L mol^{-1} cm^{-1}) and 284 nm (ϵ 18 000) in dichloromethane. The higher energy band moves to 298 nm in toluene solution, and band intensity slowly decreases over a period of several minutes. The molybdenum complex shows characteristic bands at 678 and 516 nm in CH_2Cl_2, which move to 688 and 534 nm in toluene. Spectral changes occur rapidly after solution preparation; accurate values for extinction coefficients were impossible to obtain. Spectral changes may be due to decomposition in solution; however, from the solid-state stability of the complexes this seems unlikely. A monomer–dimer equilibrium also seems unlikely with the strong bonds to the bridging catecholate oxygens. Disruption of the solvate structure is a strong possibility and may account for the solvent dependence of the spectra.

Electrochemistry of $Mo_2(Cl_4Cat)_6$ and $W_2(Cl_4Cat)_6$. Both $Mo_2(Cl_4Cat)_6$ and $W_2(Cl_4Cat)_6$ show a rich electrochemistry. The reduction series for the molybdenum complex is shown in Figure 3; potentials for both complexes are given in Table IV. Con-

Table IV. Voltammetric Redox Processes for $Mo_2(Cl_4Cat)_6$ and $W_2(Cl_4Cat)_6$

	$E°$, V (ΔE_p, mV)	
	$Mo_2(Cl_4Cat)_6$	$W_2(Cl_4Cat)_6$
redn 1	−0.26 (67)[a]	−1.00 (78)
redn 2	−0.67 (65)	−1.24 (87)
redn 3	−1.70 (95)	−1.40 (107)
oxidn 1[b]	+0.85	+1.20
oxidn 2	+1.09	+1.48
oxidn 3	+1.49	
oxidn 4	+1.67	

[a] $E°$ values recorded at a scan rate of 200 mV/s and referenced to the Fc/Fc^+ couple. [b] All oxidations were observed to be irreversible.

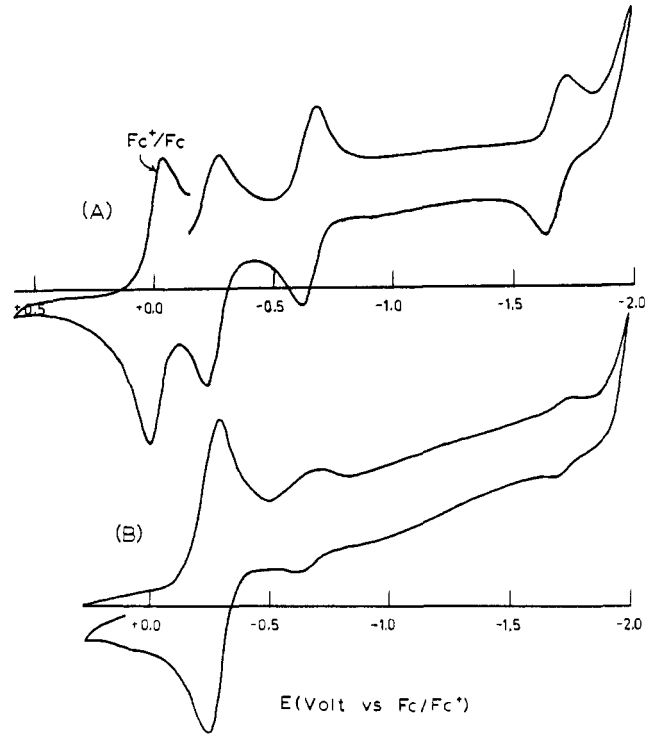

Figure 3. Cyclic voltammograms showing the two-electron-reduction couples of $Mo_2(Cl_4Cat)_6$ in the presence of ferrocene (A) and in the absence of ferrocene (B). CV's were recorded in CH_2Cl_2 at a scan rate of 200 mV/s.

trolled-potential coulometry was used to measure the current associated with the reduction processes. Reduction of the molybdenum complex occurs in three reversible two-electron steps at potentials of −0.26, −0.67, and −1.70 V (vs Fc/Fc^+). The first two reductions of the tungsten complex are shifted to negative potentials, −1.00 and −1.24 V, and the series is spread over a more narrow range of values. The third reduction occurs at −1.40 V, positive with respect to the corresponding third reduction step of the Mo complex. Since the catecholate ligands are in the fully reduced form, reductions must occur at the metal ions to give first the M^V_2 complex and in the second and third processes dimers containing tetravalent and trivalent metal ions:

$$M^{VI}_2(Cl_4Cat)_6 \overset{2e^-}{\rightleftharpoons} M^{V}_2(Cl_4Cat)_6 \overset{2e^-}{\rightleftharpoons} M^{IV}_2(Cl_4Cat)_6 \overset{2e^-}{\rightleftharpoons} M^{III}_2(Cl_4Cat)_6 \quad (1)$$

M = Mo, W

No changes in electrochemical activity were observed to occur with time, in contrast with the case of the electronic spectra. However, an unusual dependence upon the presence of ferrocene was observed in voltammetric scans for the current of the second and third reductions. This is shown in Figure 3 for the Mo complex, and it was duplicated by using both Pt-wire and glassy-carbon electrodes. In the absence of ferrocene the current of the more negative reductions was significantly lower than the

(7) Pierpont, C. G.; Buchanan, R. M. *Coord. Chem. Rev.* **1981**, *38*, 45.
(8) Cass, M. E.; Gordon, N. R.; Pierpont, C. G. *Inorg. Chem.* **1986**, *25*, 3692.

current of the first. With ferrocene in the solution potentials remained unchanged but current increased to approximately the same value as in the first reduction. The origin of this effect remains unclear, but it appears that absorbed ferrocene on the electrode surface is providing a more effective medium for electron transfer for the second and third reduction steps. Ferrocene is known to form charge-transfer interactions with quinoid organic molecules,[9] the $M_2(Cl_4Cat)_6$ complex molecules have a strong tendency to form aromatic solvates, and ferrocene-complex interactions at the electrode surface may facilitate electrode-complex electron transfer.

Beshouri and Rothwell have reported irreversible reductions for the dimeric methyl- and *tert*-butylcatecholate complexes $W_2(MeCat)_6$ and $W_2(t\text{-}BuCat)_6$ at potentials that are similar to that of the first reduction of $W_2(Cl_4Cat)_6$.[10] The irreversibility was due to dimer dissociation; the reversibility of the reductions of the $M_2(Cl_4Cat)_6$ complexes is evidence for the absence of dimer dissociation upon reduction.

Scanning to positive potentials, we observed both complexes to undergo irreversible oxidations that were accompanied by adsorption of oxidized species on the electrode surface. Oxidation must occur at the ligands as catecholate oxidation to semiquinone with complex decomposition. Potentials for the first oxidation reactions are considerably more positive than that of the Cl_4Cat/Cl_4SQ couple for the uncomplexed catechol. The extent of this shift has been viewed as a measure of the strength of the metal-bonding interaction for similarly coordinated catecholate ligands.[11] The more strongly bonded bridging ligands in the two molecules would be expected to undergo oxidation at potentials that are more positive than the oxidation potentials of the chelating ligands. Results of the structure determinations on the Mo and W complexes show that there is essentially no difference in the average M–O bond lengths for the chelated ligands, 1.949 (6) Å for $Mo_2(Cl_4Cat)_6$ and 1.941 (4) Å for $W_2(Cl_4Cat)_6$, and that these values compare well with the average Re–O length of 1.938 (5) Å for $Re(Cl_4Cat)_3$.[1] All three complexes show first oxidation reactions at similar potentials, +0.85 (Mo), +0.94 (Re), and +1.20 V (W), and these reactions appear to involve the chelated ligands.

Discussion

Reaction between $W(CO)_6$ and Cl_4BQ proceeds slowly under thermal conditions to give the $W_2(Cl_4Cat)_6$ dimer. With the more easily displacable mesitylene ligand, the analogous reaction with (mesitylene)$W(CO)_3$ should occur much more rapidly.[4] The olefin-metathesis reactions carried out for mixtures of this complex with Cl_4BQ likely involve a tetrachlorocatecholate complex of tungsten. Basset has noted that catalytic activity of tungsten(VI) phenolate complexes increases with acidity of the phenol.[3] This pattern may be carried over to the catecholate complexes, and the organometallic chemistry of $W_2(Cl_4Cat)_6$ merits investigation.

A question remains concerning effects that are responsible for the structural difference between $W_2(Cl_4Cat)_6$ and $Re(Cl_4Cat)_3$. The catecholate ligands are unique in their ability to stabilize unusually high oxidation state forms of second- and third-row transition metals without the presence of oxo ligands. The average M–O bond lengths for chelated catecholate ligands in complexes of this type fall in a narrow range: 1.941 (4) Å in $W_2(Cl_4Cat)_6$, 1.949 (6) Å in the Mo analogue $Mo_2(Cl_4Cat)_6$,[5] 1.938 (5) and 1.932 (4) Å in the monomeric rhenium(VI) complexes $Re(Cl_4Cat)_3$ and $Re(DBCat)_3$,[1] and 1.95 (1) Å in both $Os(Cat)_3$ and $Os(DBCat)_3$.[12] These M–O lengths are all relatively short and show the effect of significant π donation by catecholate ligands. Of the metals in this series, only Mo and W are d^0 and have empty t_{2g} levels for most effective π donation. This contributes to the prevalence of *cis*-dioxomolybdenum(VI) and -tungsten(VI) complexes and may account for structural differences between the tris(catecholato)molybdenum(VI) and -tungsten(VI) complexes of this series relative to the catecholate complexes of Re(VI) and Os(VI). It is also in accord with Rothwell's observed dimer dissociation for $W_2(MeCat)_6$ and $W_2(t\text{-}BuCat)_6$ upon reduction of the metal ions from d^0 to d^1. Structurally, this view is supported by the shorter cis Mo–O and W–O lengths involving the oxygens of the bridging ligands. The nonplanarity of the M–Cat–M bridges gives oxygen atoms of these ligands more aryloxide character than that of the chelated catecholate oxygens, facilitating stronger π donation to the metal.

Acknowledgment. This research was supported by the National Science Foundation under Grants CHE 85-03222 and CHE 88-09923. We thank Professor Edward McNelis for making us aware of his olefin metathesis results.

Registry No. $W(CO)_6$, 14040-11-0; $W_2(Cl_4Cat)_6 \cdot 3C_6H_5CH_3$, 116407-63-7; $Mo_2(Cl_4Cat)_6$, 56026-73-4; $W_2(Cl_4Cat)_6$, 54162-26-4; $Mo^V{}_2(Cl_4Cat)_6$, 116437-07-1; $W^V{}_2(Cl_4Cat)_6$, 116437-05-9; $Mo^{IV}{}_2(Cl_4Cat)_6$, 116437-08-2; $W^{IV}{}_2(Cl_4Cat)_6$, 116466-62-7; $Mo^{III}{}_2(Cl_4Cat)_6$, 116437-09-3; $W^{III}{}_2(Cl_4Cat)_6$, 116437-06-0; tetrachloro-1,2-benzoquinone, 2435-53-2.

Supplementary Material Available: For $W_2(Cl_4Cat)_6$, a table giving crystal data and details of the structure determination, tables of dihedral angles, least-squares planes, anisotropic thermal parameters, and coordinates for toluene solvate molecules, and a stereoview of the complex molecule (10 pages); a listing of observed and calculated structure factors (49 pages). Ordering information is given on any current masthead page.

(9) Miller, J. S.; Zhang, J. H.; Reiff, W. M. *J. Am. Chem. Soc.* **1987**, *109*, 4584.
(10) Beshouri, S. M.; Rothwell, I. P. *Inorg. Chem.* **1986**, *25*, 1962.
(11) Bradbury, J. R.; Schultz, F. A. *Inorg. Chem.* **1986**, *25*, 4416.
(12) Nielson, A. J.; Griffith, W. P. *J. Chem. Soc., Dalton Trans.* **1978**, 1501.